

Airway epithelial interferon response to SARS-CoV-2 is inferior to rhinovirus and heterologous rhinovirus infection suppresses SARS-CoV-2 replication

Elizabeth R. Vanderwall¹, Kaitlyn A. Barrow¹, Lucille M. Rich¹, David F. Read², Cole Trapnell², Oghenemega Okoloko¹, Steven F. Ziegler³, Teal S. Hallstrand⁴, Maria P. White¹, Jason S. Debley^{1,5}

¹ Center for Immunity and Immunotherapies. Seattle Children's Research Institute, Seattle, WA., USA.

² Department of Genome Sciences. University of Washington, Seattle, WA., USA.

³ Center for Fundamental Immunology, Benaroya Research Institute at Virginia Mason, Seattle, Washington; Department of Immunology, University of Washington School of Medicine, Seattle, Washington.

⁴ Division of Pulmonary, Critical Care, and Sleep Medicine and the Center for Lung Biology, University of Washington, Seattle, WA., USA.

⁵ Department of Pediatrics, Division of Pulmonary and Sleep Medicine, Seattle Children's Hospital, University of Washington, Seattle, WA., USA.

Corresponding Author: Jason.debley@seattlechildrens.org; Jason S. Debley, MD, MPH, ORCID ID: <https://orcid.org/0000-0001-6438-9535>, ADDRESS: Center for Immunity and Immunotherapies, Seattle Children's Research Institute, 1900 Ninth Ave., Seattle, WA, 98145

Author Contributions: Conceptualization, K.A.B., C.T., J.S.D.; methodology, K.A.B., E.R.V., L.M.R., O.O., J.S.D.; validation, E.R.V., L.M.R., K.A.B., J.S.D.; formal analysis, E.R.V., J.S.D.; investigation, E.R.V., L.M.R., K.A.B., M.P.W., O.O., J.S.D.; resources, T.S.H., J.S.D.; data curation, O.O., K.A.B., L.M.R., M.P.W., E.R.V., J.S.D.; writing—original draft preparation, E.R.V., J.S.D.; writing—review and editing, E.R.V., L.M.R., M.P.W., O.O., S.F.Z., T.S.H., D.F.R., C.T., K.A.B., J.S.D.; supervision, J.S.D.; project administration, J.S.D.; funding acquisition, S.F.Z., J.S.D. All authors have read and agreed to the published version of the manuscript.

Supported by: NIH NIAID K24AI150991-01S1 (JSD); U19AI125378-05S1 (SFZ, JSD)

Word Count: Body: 4287; Abstract: 254

Key words: SARS-CoV-2, COVID-19, rhinovirus, airway epithelial cells, epithelium, interferon, children, adults

ABSTRACT

Introduction: Common alphacoronaviruses and human rhinoviruses (HRV) induce type I and III interferon (IFN) responses important to limiting viral replication in the airway epithelium. In contrast, highly pathogenic betacoronaviruses including SARS-CoV-2 may evade or antagonize RNA-induced IFN I/III responses. **Methods:** In airway epithelial cells (AECs) from children and older adults we compared IFN I/III responses to SARS-CoV-2 and HRV-16, and assessed whether pre-infection with HRV-16, or pretreatment with recombinant IFN- β or IFN- λ , modified SARS-CoV-2 replication. Bronchial AECs from children (ages 6-18 yrs.) and older adults (ages 60-75 yrs.) were differentiated *ex vivo* to generate organotypic cultures. In a biosafety level 3 (BSL-3) facility, cultures were infected with SARS-CoV-2 or HRV-16, and RNA and protein was harvested from cell lysates 96 hrs. following infection and supernatant was collected 48 and 96 hrs. following infection. In additional experiments cultures were pre-infected with HRV-16, or pre-treated with recombinant IFN- β 1 or IFN- λ 2 before SARS-CoV-2 infection. **Results:** Despite significant between-donor heterogeneity SARS-CoV-2 replicated 100 times more efficiently than HRV-16. IFNB1, INFL2, and CXCL10 gene expression and protein production following HRV-16 infection was significantly greater than following SARS-CoV-2. IFN gene expression and protein production were inversely correlated with SARS-CoV-2 replication. Treatment of cultures with recombinant IFN β 1 or IFN λ 2, or pre-infection of cultures with HRV-16, markedly reduced SARS-CoV-2 replication. **Discussion:** In addition to marked between-donor heterogeneity in IFN responses and viral replication, SARS-CoV-2 elicits a less robust IFN response in primary AEC cultures than does rhinovirus, and heterologous rhinovirus infection, or treatment with recombinant IFN- β 1 or IFN- λ 2, markedly reduces SARS-CoV-2 replication.

1 INTRODUCTION

2 The novel coronavirus SARS-CoV-2 has rapidly infected humans across the globe,
3 causing one of the most devastating pandemics in modern history, with over 240 million
4 confirmed cases and nearly 5 million deaths worldwide by October 2021(1). While most cases
5 of the resulting coronavirus disease 2019 (COVID-19) are mild, some cases are severe and
6 complicated by respiratory and multi-organ failure(2), with a fatality rate ranging from as low as
7 0.2% to as high as 27% depending on underlying medical co-morbidity and age(3). For the first
8 half of the pandemic, incidence of COVID-19 was surprisingly low among children(3), however,
9 there is evidence that SARS-CoV-2 infection rates are as high in children as older adults(3) and
10 that children can shed SARS-CoV-2 while asymptomatic and for prolonged periods(4). More
11 recently, the incidence of COVID-19 in the United States has increased significantly among
12 children and adolescents(5). Understanding mechanisms that explain the heterogeneity of
13 severity with SARS-CoV-2 infection between individuals and across different age groups may
14 assist efforts to develop therapeutic interventions to treat and prevent COVID-19.

15 One potential explanation for the wide variation in COVID-19 disease severity is the
16 differences in the innate immunity between individuals, particularly the heterogeneity of type I
17 and III interferon (IFN) responses. Innate immune sensing of coronaviruses, including SARS-
18 CoV-2, is thought to occur primarily through pattern recognition receptors (PRRs) including the
19 cytosolic RIG-I-like receptors, melanoma differentiation-associated protein 5 (MDA5; coded for
20 by the gene *IFIH1*), and retinoic acid-inducible gene I (RIG-I) as well as cell surface or
21 endosomal transmembrane toll-like receptors (TLRs) TLR3 and TLR7, which lead to the
22 activation of signaling cascades that further induce type I and III IFN responses(6) (7) (8) (9).
23 Common human coronavirus (HCoV) strains (e.g. alpha-coronavirus strain 229E) potently
24 induce type I and III IFN, and their replication is susceptible to inhibition by IFN I/III, leading to
25 suppression of the early phase of viral replication(10) (11). In contrast, previous highly

26 pathogenic beta-HCoVs (e.g. SARS-CoV and MERS-CoV) encode viral proteins with a greater
27 capability to antagonize RNA-induced type I and III IFN production through perturbation of RNA
28 sensing(12) (13) (14) (15) (16) (17). Likewise, IFN responses at mucosal surfaces appear to be
29 muted during SARS-CoV-2 infection as compared to other respiratory viruses, suggesting
30 evasion of innate immune responses by SARS-CoV-2(18) (19). Data from our lab and others
31 indicates that epithelial infection with human rhinovirus increases the expression of the entry
32 receptors for SARS-CoV-2(20) (21), suggesting that when these two viruses concurrently infect
33 individuals the response to one virus could modulate the response to the other.

34 Data from clinical studies increasingly support a hypothesis that deficiency of initial IFN
35 responses to SARS-CoV-2 may allow for increased viral replication that then supports systemic
36 inflammatory responses that contribute to COVID-19 pathology and severity(19) (22) (23) (24).
37 Ziegler et al. recently performed scRNA-seq on nasopharyngeal swabs from 15 healthy adults,
38 14 adults with mild COVID-19 and 21 adults with severe COVID-19, and observed that epithelial
39 cells from patients with severe COVID-19 had less robust expression of anti-viral interferon
40 response genes as compared to patients with mild COVID-19 and healthy controls supporting
41 their conclusion that a “failed” nasal epithelial innate anti-viral response may be a risk factor for
42 severe COVID-19(25).

43 The objectives of our study were to determine if heterogeneity in bronchial epithelial type
44 I and III IFN responses to SARS-CoV-2 between individual pediatric and adult donors was
45 associated with SARS-CoV-2 replication, to compare airway epithelial IFN responses between
46 SARS-CoV-2 and human rhinovirus-A16 (HRV-16), and to determine the effects of HRV pre-
47 infection or exogenous IFN treatment on SARS-CoV-2 replication in organotypic airway
48 epithelial cell (AEC) cultures from children and adults. We hypothesized that type I and III IFN
49 responses would be less vigorous to SARS-CoV-2 than to HRV infection, that IFN responses
50 would be associated with SARS-CoV-2 replication, and that HRV pre-infection and/or

51 recombinant IFN treatment of airway epithelial cultures would decrease replication of SARS-
52 CoV-2. Some of the results of these studies have been previously reported in the form of an
53 abstract(26).

54

55 **METHODS**

56 Bronchial AECs from children ages 6-18 years (n=15) and older adults ages 60-75 years
57 (n=10) were differentiated *ex vivo* at an air-liquid interface (ALI) to generate organotypic
58 cultures. AECs from children were obtained under study #12490 approved by the Seattle
59 Children's Hospital Institutional Review Board. Parents of subjects provided written consent and
60 children over 7 years of age provided assent. Primary bronchial AECs from adults were
61 purchased from Lonza® or obtained from a tracheal segment lung transplant donor lung tissue.
62 AECs were differentiated *ex vivo* for 21 days at an ALI on 12-well collagen-coated Corning®
63 plates with permeable transwells in PneumaCult™ ALI media (Stemcell™) at 37°C in an
64 atmosphere of 5% CO₂ as we have previously described, producing an organotypic
65 differentiated epithelial culture with mucociliary morphology(27) (28) (29) (30).

66 Experimental conditions in this study included: infection of AECs with SARS-CoV-2
67 alone, infection of AECs with HRV-16 alone, infection of AECs with HRV-16 followed by
68 infection with SARS-CoV-2 72 hours later, infection of IFNβ1 treated AECs with SARS-CoV-2,
69 and infection of IFNλ2 treated AECs with SARS-CoV-2. For AECs treated with recombinant IFN,
70 recombinant IFNβ1 (1ng/mL) or IFNλ2 (10ng/mL) was added to basolateral transwell chamber
71 with every medium change, starting 72 hours prior to SARS-CoV-2 infection and continuing until
72 96 hours following SARS-CoV-2 infection. The concentrations of recombinant IFNβ1 and IFNλ2
73 were chosen based on data from preliminary experiments in three primary AEC lines comparing
74 the effect of a range of concentrations of each cytokine from 0.1 - 10 ng/mL on SARS-CoV-2

75 replication (data not shown). In a Biosafety Level 3 (BSL-3) facility, cultures were infected with
76 SARS-CoV-2 isolate USA-WA1/2020 or HRV-16 at a multiplicity of infection (MOI) of 0.5. At 96
77 hrs. following SARS-CoV-2, or following HRV-16 infection alone, RNA was isolated from cells
78 using Trizol® and protein was isolated from cell lysates with RIPA buffer (Sigma-Aldrich®)
79 containing Triton X100 1% and SDS 0.1%, methods that we have demonstrated fully inactivate
80 SARS-CoV-2(31).

81 Expression of *IFNB1*, *IFNL2*, *CXCL10*, *IFIH1*, and *GAPDH* were measured by
82 quantitative polymerase chain reaction (qPCR) using Taqman® probes. To measure SARS-
83 CoV-2 replication in AEC cultures we used the Genesig® Coronavirus Strain 2019-nCoV
84 Advanced PCR Kit (Primerdesign®), with duplicate assays of harvested RNA from each SARS-
85 CoV-2-infected AEC experimental condition. The viral copy number used in analyses of each
86 experimental condition was the mean of duplicate assays from each experimental condition.
87 Similarly, to measure HRV-16 replication in AEC cultures we used the Genesig® Human
88 Rhinovirus Subtype 16 PCR Kit (Primerdesign®).

89 To extract protein from the cell layer of SARS-CoV-2-infected AEC cultures, media was
90 first removed from the basolateral chamber of transwells. Next, 100 µL of cold PBS was added
91 to the apical surface of cultures and 1mL was added to the basolateral chamber of cultures as a
92 wash step. Next, 50µL of RIPA buffer for protein extraction ready-to-use-solution (Sigma-
93 Aldrich®, Product No. R0278) containing Triton X100 1% and SDS 0.1% was added to the
94 apical surface of AECs and incubated for 15 minutes on ice. A pipet tip was then used to gently
95 scratch each apical well in a crosshatch pattern to loosen AECs from the transwell membrane.
96 Material was collected, centrifuged at 10,000 rpm at 4°C for 10 minutes, then supernatant
97 containing isolated protein was collected. IFNβ1, IFNλ2, and CXCL-10 protein concentrations in
98 cell lysates, and IFNβ1, IFNλ3, and CXCL-10 concentrations were measured in cell culture

99 supernatants, via a Human Luminex® Assay (R&D®), with protein concentrations normalized to
100 total protein levels in lysate (BCA assay; Sigma-Aldrich®).

101 **Statistical Analysis**

102 Gene expression and protein levels are presented as means +/- standard deviation (SD)
103 when data were normally distributed, and as medians with interquartile range if one or more
104 groups were not normally distributed. To determine if data was normally distributed the
105 Kolmogorov-Smirnov test was used ($\alpha = 0.05$). *IFNB1*, *IFNL2*, *IFIH1* and *CXCL10* relative
106 expression were standardized using *GAPDH* as a non-regulated housekeeping gene. GenEx
107 version 5.0.1 was used to quantify gene expression from qPCR normalized to *GAPDH* (MultiD
108 Analyses AB, Göteborg, Sweden) based on methods described by Pfaffl(32). Data in at least
109 one group or condition in each experiment analyzed were determined to be non-normally
110 distributed, therefore nonparametric tests were used for analyses. To compare gene expression
111 data and distributions of protein concentrations in cell lysates and supernatants between paired
112 groups the Wilcoxon matched-pairs signed rank test was used. For unpaired data the Mann-
113 Whitney test was used for analyses. For experiments with three or more conditions the Kruskal-
114 Wallis one-way ANOVA on ranks test was used, and *post hoc* comparisons between pairs of
115 subject groups were made using Dunn's multiple comparisons test (significance level set at
116 $p < 0.05$). Correlations were determined using the Spearman's rank correlation coefficient. Data
117 was analyzed using Prism® 9.0 software (GraphPad Software Inc., San Diego, CA.). Statistical
118 significance was set at $p < 0.05$.

119

120 **RESULTS**

121 In organotypic primary bronchial AEC cultures from children (n=15) and older adults
122 (n=10) we observed marked heterogeneity in SARS-CoV-2 replication between human donors

123 (Figure 1). The clinical characteristics of human airway epithelial donors included in these
124 experiments is summarized in Table 1. Despite the significant between-subject heterogeneity in
125 SARS-CoV-2 replication, we observed that SARS-CoV-2 replicated approximately 100 times
126 more efficiently than HRV-16 in these primary bronchial AEC cultures (Figure 1; SARS-CoV-2
127 median copy number 215,387 vs. HRV-16 median copy number 2211; $p < 0.0001$) when parallel
128 cultures from each donor were infected with each virus at the same MOI of 0.5. When data
129 from pediatric and adult cultures were analyzed separately SARS-CoV-2 replication was also
130 markedly greater than HRV-16 in cultures within each donor age group (children: SARS-CoV-2
131 median copy number 215,387 vs. HRV-16 median copy number 2602; $p < 0.001$; adults: SARS-
132 CoV-2 median copy number 75,940 vs. HRV-16 median copy number 2184; $p = 0.002$). SARS-
133 CoV-2 replication was not significantly different between AEC cultures from pediatric and adult
134 donors (median copy number 215,387 vs. 75,940; $p = 0.23$), and among pediatric donors SARS-
135 CoV-2 replication was not significantly different between cultures from children with asthma and
136 healthy children (median copy number 60,540 vs. 436,465; $p = 0.3$).

137 For primary bronchial epithelial cultures wherein SARS-CoV-2 and HRV-16 infection was
138 compared in parallel, RNA harvested 96 hours following infection was available from 22 donor
139 cultures ($n = 14$ children, $n = 8$ adults) to allow measurement of *IFNB1*, *IFNL2*, and *CXCL10* gene
140 expression, and protein was available from cell lysate collected 96 hours following infection from
141 20 donor cultures ($n = 12$ children, $n = 8$ adults) to allow for measurement of $IFN\beta 1$, $IFN\lambda 2$ (IL-
142 28A), and CXCL-10 protein levels. As compared to uninfected cultures, the relative increase in
143 expression of *IFNB1* following infection with HRV-16 was significantly greater than following
144 infection with SARS-CoV-2 (median increase expression 4.4-fold vs. 1.4-fold, $p < 0.0001$; Figure
145 2, panel A). Similarly, the relative increase in expression of *IFNL2* following infection with HRV-
146 16 was significantly greater than following infection with SARS-CoV-2 (median increase
147 expression 21.2-fold vs. 4.3-fold, $p < 0.0001$; Figure 2, panel C), as was the increase in

148 expression of *CXCL10* (median increase expression 9.8-fold vs. 5.4-fold, $p=0.003$; Figure 2,
149 panel E). The expression of these three genes was significantly greater following HRV-16
150 infection than following SARS-CoV-2 in cultures from both children and adults when analyzed
151 separately (data not shown). The concentrations of IFN β 1, IFN λ 2 (IL-28A), and CXCL-10
152 protein, normalized to total protein concentration, in cell lysates collected 96 hours following
153 infection with HRV-16 were also significantly greater than in parallel cultures following SARS-
154 CoV-2 infection (IFN β 1: median 892 vs. 663 pg/mL, $p=0.02$, Figure 2, panel B; IFN λ 2 (IL-28A):
155 9848 vs. 7123 pg/mL, $p=0.02$, Figure 2, panel D; and CXCL-10: 69,306 vs. 15,232 pg/mL,
156 $p<0.0001$, Figure 2, panel F).

157 Of cultures wherein SARS-CoV-2 and HRV-16 infection was compared in parallel,
158 supernatant was collected from $n=16$ donor cell lines 48 hours following infection and from $n=20$
159 cell lines 96 hours following infection. Concentrations of IFN β 1 in supernatant (normalized to
160 total protein concentration) were higher at 48 hours vs. 96 hours post infection for both viruses.
161 However, IFN β 1 concentrations were significantly greater following HRV-16 as compared to
162 SARS-CoV-2 infection at both 48 hours (median 60.4 vs. 12.5 pg/mL, $p<0.001$, Figure 3, panel
163 A) and 96 hours (median 7.1 vs. 1.4 pg/mL, $p<0.001$, Figure 3, panel A). IFN λ 2 (IL-28A)
164 concentrations were below the assay detection level in supernatants for most samples (data not
165 shown). IFN λ 3 (IL-28B) concentrations in supernatants were significantly greater following HRV-
166 16 as compared to SARS-CoV-2 infection at both 48 hours (median 1335 vs. 40.6 pg/mL,
167 $p<0.001$, Figure 3, panel B) and 96 hours (median 197 vs. 48 pg/mL, $p<0.001$, Figure 3, panel
168 B). CXCL10 concentrations in supernatants were also significantly greater following HRV-16 as
169 compared to SARS-CoV-2 infection at both 48 hours (median 293,805 vs. 10,407 pg/mL,
170 $p<0.001$, Figure 3, panel C) and 96 hours (median 179,858 vs. 150,939 pg/mL, $p=0.04$, Figure
171 3, panel C).

172 At 96 hours following infection we assessed correlations between relative expression of
173 *IFNB1* and *IFNL2* in individual primary bronchial epithelial cell lines and viral replication (SARS-
174 CoV-2 copy number) in those cultures. Both *IFNB1* and *IFNL2* gene expression was inversely
175 correlated with SARS-CoV-2 replication (*IFNB1* $r=-0.61$, $p=0.003$; *IFNL2* $r=-0.42$, $p=0.05$; Figure
176 4). Because concentrations of IFN β 1 and IFN λ 3 in supernatants were highest at 48 hours
177 following infection, we assessed correlations between supernatant concentrations of these
178 cytokines at 48 hours following SARS-CoV-2 infection and viral replication at 96 hours following
179 infection and observed a significant inverse correlation between supernatant IFN β 1
180 concentrations and viral replication ($r=-0.53$, $p=0.02$; Figure 5, panel A) and a trend toward an
181 inverse correlation between supernatant IFN λ 3 concentrations and viral replication ($r=-0.44$,
182 $p=0.06$, data not shown). We observed significant negative correlations between CXCL10
183 protein concentrations in both supernatant ($r=-0.56$, $p=0.01$, data not shown) and cell lysate ($r=-$
184 0.65 , $p=0.002$; Figure 5, panel B) at 96 hours following infection and SARS-CoV-2 replication.

185 In organotypic bronchial epithelial cultures from 14 children and 10 older adults,
186 replication of SARS-CoV-2 was compared between cultures infected with SARS-CoV-2 alone
187 (MOI=0.5), infection of cultures with HRV-16 (MOI=0.5) followed 72 hours later by infection with
188 SARS-CoV-2 (MOI=0.5), infection of IFN β 1 pre- and concurrently treated cultures with SARS-
189 CoV-2, and infection of IFN λ 2 pre- and concurrently treated cultures with SARS-CoV-2. Pre-
190 infection of bronchial AECs with HRV-16 led to a marked reduction in SARS-CoV-2 replication
191 96 hours following infection (median SARS-CoV-2 copy number 267,264 vs. 14,788, $p=0.002$;
192 Figure 6). Treatment of AEC cultures with recombinant IFN β 1 reduced SARS-CoV-2 replication
193 from a median copy number of 267,264 to 11,947 ($p=0.0001$) and treatment of AEC cultures
194 with recombinant IFN λ 2 reduced SARS-CoV-2 replication from a median copy number of
195 267,264 to 11,856 ($p=0.0002$).

196 Given that SARS-CoV and MERS have been noted to evade innate antiviral defenses at
197 various steps between viral sensing and transcription and translational of type I and III
198 interferons, and ultimately transcription of an array antiviral genes(12) (13) (14) (15) (16) (17),
199 we assessed one potential proximal step where SARS-CoV-2 may evade sensing of viral
200 nucleic acids by comparing gene expression of the pattern-recognition receptor and RNA viral
201 sensor IFIH1/MDA5 between primary bronchial AEC cultures infected in parallel with SARS-
202 CoV-2 (MOI=0.5) or HRV-16 (MOI=0.5). We observed that IFIH1 expression was more than 2-
203 fold greater following infection with HRV-16 as compared to following SARS-CoV-2 infection
204 (Figure 7; p=0.003).

205

206 **DISCUSSION**

207 A growing body of literature suggests that beta-HCoVs, including SARS-CoV-2 appear
208 able to antagonize type I and III IFN responses at mucosal surfaces at multiple steps between
209 viral sensing and production of interferon induced antiviral proteins(18) (19) (33). In this study
210 we directly compared type I and III IFN responses to SARS-CoV-2 and HRV-16 infection by
211 primary organotypic bronchial AEC cultures from children and adults, and assessed the impact
212 of exogenous treatment with recombinant IFN β 1 or IFN λ 2 on SARS-CoV-2 replication as well as
213 the impact of heterologous infection with HRV-16 prior to SARS-CoV-2. We observed significant
214 heterogeneity in SARS-CoV-2 replication between primary AEC lines from different human
215 donors, however, despite between donor heterogeneity we also observed that SARS-CoV-2
216 replicated approximately 100 times more efficiently than HRV-16 in these primary bronchial
217 AEC cultures. As compared to uninfected cultures, the relative increase in expression of *IFNB1*,
218 *INFL2*, and *CXCL10* following infection with HRV-16 was significantly greater than following
219 infection with SARS-CoV-2, and the protein concentrations of type I and III IFN and the IFN

220 stimulated chemokine CXCL10 in both cell lysates and supernatant were significantly greater in
221 AEC cultures following infection with HRV-16 as compared to SARS-CoV-2. In SARS-CoV-2
222 infected AEC cultures type I and III IFN gene expression and protein production were inversely
223 correlated with viral replication. Furthermore, treatment of AEC cultures with recombinant IFN β 1
224 or IFN λ 2, or pre-infection of AEC cultures with HRV-16, markedly reduced SARS-CoV-2
225 replication.

226 Sensing of beta-HCoVs by the innate immune system is believed to be primarily through
227 pattern recognition receptors (PRRs), including cell surface or endosomal transmembrane TLRs
228 TLR3 and TLR7, the cytosolic RIG-I-like receptors melanoma differentiation-associated protein
229 5 (MDA5), as well as retinoic acid-inducible gene I (RIG-I) (6) (7) (8) (9). PRR's then mediate
230 activation of signaling cascades leading to induction of type I and III IFN responses(6) (7) (8)
231 (9). Recently Sampaio et al. reported that in the lung cancer cell line Calu-3 the cytosolic RNA
232 sensor MDA5 was required for type I and III IFN induction when cells were infected with SARS-
233 CoV-2 infection(6).

234 Studies using immortalized cell lines (e.g. Vero, HeLa, Calu-3, 293T) *in vitro*, as well as
235 murine *in vivo* studies, have suggested a number of potential mechanisms by which beta-
236 HCoVs (e.g. SARS-CoV, MERS-CoV, and SARS-CoV-2) may evade IFN responses at the level
237 of the airway epithelium. Prior to the onset of the COVID-19 pandemic, these mechanisms were
238 investigated extensively for SARS-CoV and MERS-CoV. One group of beta-HCoV proteins, the
239 predominantly non-structural proteins (nsps), are recognized to have IFN-antagonistic impacts.
240 Several nsps (e.g. nsp1 and nsp3) interfere with signal transduction mediated by PRRs, while
241 other nsps evade recognition by PRRs in mucosal epithelial cells by modifying features of the
242 viral RNA(34). There is growing evidence that SARS-CoV-2, much like SARS-CoV and MERS-
243 CoV, has evolved a number of immune evasion strategies that may interfere with PRR's
244 themselves(35) (36) (37) (38) (39) (40) (41) (42), inhibit multiple steps in the signaling cascade

245 leading to induction and translation of type I and III IFNs(43) (44) (45) (46) (47) (48) (49) (50)
246 (51) (52), and interfere with the actions of IFNs by impeding the signaling pathways that lead to
247 transcription and translation of anti-viral interferon stimulated genes (ISGs) (18) (53) (54) (55)
248 (56). Lei et al. demonstrated that the SARS-CoV-2 proteins NSP1, NSP3, NSP12, NSP13,
249 NSP14, ORF3, ORF6 and M protein all have some ability to inhibit Sendai virus-induced IFN- β
250 promoter activation, and that ORF6 has inhibitory effects on both type I IFN production as well
251 as signaling downstream of IFN- β production(18). Early in the COVID-19 pandemic Blanco-Melo
252 et al. reported results from a transcriptome profiling study of various immortalized cell lines
253 which demonstrated that SARS-CoV-2 infection elicited very low type I and III IFN and limited
254 ISG responses, while inducing expression of pro-inflammatory cytokines genes(19), raising the
255 possibility that a deficient epithelial IFN response to SARS-CoV-2 may facilitate enhanced local
256 viral replication that ultimately might lead to a dysregulated systemic pro-inflammatory
257 response.

258 Data from several clinical studies have provided additional support for the hypothesis
259 that a muted initial local IFN response to SARS-CoV-2 in the airway epithelium, at least in some
260 hosts, allows the virus to replicate unimpeded which then sets up the host for potential systemic
261 inflammatory responses that contribute to COVID-19 pathology and severity(19) (22) (23) (24).
262 Recently, Ziegler et al. published transcriptomics results from nasopharyngeal swabs from 15
263 healthy adults, 14 adults with mild COVID-19 and 21 adults with severe COVID-19, and
264 observed that nasal epithelial cells from patients with severe COVID-19 exhibited less robust
265 expression of anti-viral IFN response genes as compared to patients with mild COVID-19 and
266 healthy adults, supporting their conclusion that a “failed” nasal epithelial innate anti-viral
267 response may be a risk factor for severe COVID-19(25).

268 In the early stages of the pandemic, morbidity and mortality was skewed toward older
269 patients with significant underlying comorbidities, however, over time it has become increasingly

270 clear that clinical outcomes with COVID-19 following infection with SARS-CoV-2 is
271 heterogeneous with outcomes even in young adults and children without medical comorbidities
272 unpredictably ranging from asymptomatic infection to death(57). An objective of
273 our study was to determine if heterogeneity in airway epithelial IFN responses to SARS-CoV-2
274 between individual pediatric and adult donors was associated with SARS-CoV-2 replication. A
275 striking observation in our data is the marked between-donor heterogeneity in the replication of
276 SARS-CoV-2 in organotypic AEC cultures using standardized protocols and uniform viral
277 inoculation doses. A potential important future area of investigation will be to investigate
278 possible genetic and epigenetic factors that may partially explain heterogeneity in SARS-CoV-2
279 replication in airway epithelium.

280 Our group and others have demonstrated that the SARS-CoV-2 entry receptor ACE2 is
281 an ISG(20) (21). We have demonstrated that HRV-16 infection induces a type I and III
282 interferon response, and increases ACE2 expression(21), leading us to originally speculate that
283 HRV pre-infection of AECs might increase replication of SARS-CoV-2 through greater
284 expression of the entry receptor and be a clinical risk factor for acquisition of COVID-19.
285 However, our results in this study demonstrate that even through the SARS-CoV-2 entry factor
286 ACE2 is an ISG, HRV-16 infection induces a much more potent type I and III IFN responses
287 than SARS-CoV-2 and that heterologous infection of organotypic AEC cultures with HRV-16
288 three days prior to inoculation with SARS-CoV-2 markedly reduces replication of SARS-CoV-2.
289 This suppression of SARS-CoV-2 replication was similar to the effects of exogenous treatment
290 with IFN β 1 or IFN λ 2, suggesting that the pronounced induction of these genes by HRV-16 was
291 responsible for these findings. These findings extend upon several other recent reports
292 including Cheemarla et al. who reported experiments in differentiated primary airway epithelial
293 cultures from small number of adult donors and observed that infection with HRV-01A prior to
294 infection with SARS-CoV-2 accelerated induction of ISGs and reduced SARS-CoV-2

295 replication(58). Similarly, Dee et al. used differentiated primary airway epithelial cultures from a
296 single human donor, to characterize viral replication kinetics of SARS-CoV-2 with and without
297 co-infection with rhinovirus and observed that pre-infection with HRV-16A reduced SARS-CoV-2
298 replication(59). Neither of these prior studies included primary ALI cultures from a robust
299 sample size of adults and children or compared interferon and ISG responses between parallel
300 HRV and SARS-CoV-2 infections in addition to HRV pre-infection to determine if this
301 phenomenon is consistent across donors with heterogenous interferon responses to both
302 viruses. Although difficult to definitely test, given that the incidence of COVID-19 in children was
303 very low in the early months of the pandemic, during the peak of the late winter viral respiratory
304 season in the United States and Europe when rhinovirus, RSV, and influenza activity was high,
305 our data together with the studies by Dee and Cheemarla (58, 59) lead us to hypothesize that
306 high rates of typical respiratory viral pathogens among Children in the northern hemisphere in
307 February-March 2020 may have contributed to protection of children early in the COVID-19
308 pandemic by generally inducing airway type I and III IFN responses.

309 Given the steady evolution of new SARS-CoV-2 variants through 2021 and continued
310 significant resistance to vaccination among a sizable minority of people with access to vaccines,
311 the pandemic has continued to result in high levels of morbidity and mortality in many areas of
312 the world, fueling an ongoing need for therapeutics to treat COVID-19. Our results
313 demonstrating marked reduction in SARS-CoV-2 replication in AEC cultures treated with
314 recombinant IFN β 1 or IFN λ 2 provides further mechanistic evidence to support the possible use
315 of inhaled interferon as a possible treatment option if initiated early enough during COVID-19. A
316 recent randomized, double-blind, placebo-controlled, phase 2 trial of inhaled nebulized
317 interferon beta-1a (SNG001) for treatment of SARS-CoV-2 infection demonstrated that patients
318 who received SNG001 early in their disease course had greater odds of improvement and

319 recovered more rapidly from SARS-CoV-2 infection than patients who received placebo,
320 providing a strong rationale for further trials of this agent(60).

321 We are not aware of other studies to date that have directly compared innate immune
322 responses between SARS-CoV-2 and HRV in organotypic AEC cultures from many pediatric
323 and adult donors. However, there are several limitations of our primary airway epithelial model
324 system. First, our *ex vivo* system lacks interaction with immune cells and the complex immune
325 responses that occur *in vivo* in the context of COVID-19, and therefore we cannot assess how
326 heterogeneity in interferon responses to SARS-CoV-2 at the level of the airway epithelium relate
327 to systemic immune responses or clinical outcomes *in vivo*. Second, in this study we did not
328 investigate potential genetic or epigenetic factors that may explain the between subject
329 heterogeneity in interferon responses and viral replication that we observed. Finally, given the
330 limitations posed by the complex logistics of completing these experiments in a biosafety level 3
331 (BSL-3) facility, together with limitations in available material from organotypic cultures from a
332 sizeable number of human donors, we were constrained in the number of feasible sample
333 harvesting timepoints which prevented us from conducting a high resolution assessment of the
334 time kinetics of viral infection and interferon responses in the present study; however, our
335 choice to harvest supernatant 48 hours following SARS-CoV-2 infection and RNA 96 hours
336 following infection was informed by both our prior work with RSV(29) and preliminary
337 experiments with SARS-CoV-2 (data not shown) where we observed that in organotypic primary
338 ALI cultures type I and III interferon responses peak between 24-48 hours while expression of
339 downstream ISGs peak between 72-96 hours.

340 In conclusion, in this study we have demonstrated that in addition to remarkable
341 between subject heterogeneity in interferon responses and viral replication, SARS-CoV-2 elicits
342 a less robust type I and III interferon response in organotypic primary bronchial AEC cultures

343 than does human rhinovirus, and that pre-infection of AECs with HRV-16, or pre-treatment with
344 recombinant IFN- β 1 or IFN- λ 2, markedly reduces SARS-CoV-2 replication.

345

346

347 **List of Abbreviations**

348 COVID-19: coronavirus disease 2019

349 IFN: interferon

350 PRR: pattern recognition receptors

351 MDA5: melanoma differentiation-associated protein 5

352 RIG-I: retinoic acid-inducible gene I

353 TLR: toll-like receptor

354 HCoV: human coronavirus

355 HRV-16: human rhinovirus-A16

356 AEC: airway epithelial cell

357 ALI: air-liquid interface

358 BSL-3: Biosafety Level 3

359 MOI: multiplicity of infection

360 qPCR: quantitative polymerase chain reaction

361

362 **Declarations**

363 **Ethics Approval:** Airway epithelial cells from children were obtained under study #12490
364 approved by the Seattle Children’s Hospital IRB. Parents of subjects provided written consent
365 and children over 7 years of age provided assent. Airway epithelial cells from adults were
366 purchased from Lonza® without personal identifiers. The Seattle Children’s Hospital IRB
367 determined that use of de-identified adult airway epithelial cells purchased from Lonza® did not
368 require ethics approval or consent.

369 **Consent for publication:** This manuscript does not contain any individual person’s data in any
370 form.

371 **Availability of data and materials:** The datasets used and/or analysed during the current
372 study are available from the corresponding author on reasonable request.

373 **Competing interests:** The authors declare that they have no competing interests.

374 **Funding:** NIH NIAID K24AI150991-01S1 (JSD); U19AI125378-05S1 (SFZ, JSD)

375 **Author Contributions:** Conceptualization, K.A.B., C.T., J.S.D.; methodology, K.A.B.,
376 E.R.V., L.M.R., O.O., J.S.D.; validation, E.R.V., L.M.R., K.A.B., J.S.D.; formal analysis,
377 E.R.V., J.S.D.; investigation, E.R.V., L.M.R., K.A.B., M.P.W., O.O., J.S.D.; resources,
378 T.S.H., J.S.D.; data curation, O.O., K.A.B., L.M.R., M.P.W., E.R.V., J.S.D.; writing—
379 original draft preparation, E.R.V., J.S.D.; writing—review and editing, E.R.V., L.M.R.,
380 M.P.W., O.O., S.F.Z., T.S.H., D.F.R., C.T., K.A.B., J.S.D.; supervision, J.S.D.; project
381 administration, J.S.D.; funding acquisition, S.F.Z., J.S.D. All authors have read and
382 agreed to the published version of the manuscript.

383 **Table 1: Airway Epithelial Cell Donor Characteristics**

	Pediatric AEC Donors (n=15)	Adult AEC Donors (n=10)
Age (yrs., mean +/- SD)	10.5 +/- 2.0	67 +/- 4.9
Gender (female)	9 (60%)	4 (40%)
Active Smoker	0 (0%)	3 (30%)
History of Asthma	8 (53%)	0 (0%)
Obesity	0 (0%)	4 (40%)
Hypertension	0 (0%)	3 (3%)

384

385 **AEC = Airway epithelial cell**

386 **Figure 1.** SARS-CoV-2 and HRV-16 replication by quantitative PCR in primary bronchial AECs
387 from children (n=15) and adults (n=10). Viral copy number was quantified by PCR in RNA
388 harvested from AEC cultures 96 hours following infection (MOI of 0.5) with either SARS-CoV-2
389 (red circles) or HRV-16 (blue triangles). SARS-CoV-2 replication was significantly greater than
390 HRV-16 (median copy number 215,387 vs. HRV-16 median copy number 2211; $p < 0.0001$ by
391 Wilcoxon matched-pairs signed rank test; bars indicate median values).

392 **Figure 2.** Relative gene expression of *IFNB1*, *IFNL2*, and *CXCL10* (normalized to GAPDH
393 expression) by primary bronchial airway epithelial cell cultures in children (n=14) and adults
394 (n=8), and parallel IFN β 1, IFN- λ 2 (IL-28a), and CXCL10 protein concentrations in cell lysates
395 (normalized to total protein concentration), from primary bronchial airway epithelial cell cultures
396 from children (n=12) and adults (n=8) harvested 96 hours after SARS-CoV-2 (red circles) or
397 HRV-16 (blue triangles) infection. Expression of *IFNB1* and corresponding concentrations of
398 IFN β 1 in cell lysates were significantly greater in cultures after infection with HRV-16 than in
399 cultures infected with SARS-CoV-2 (**Panel A**, median increase expression 4.4-fold vs 1.4-fold,
400 $p < 0.0001$; **Panel B**, median 892 pg/mL vs 663 pg/mL, $p = 0.02$). Expression of *IFNL2*, and IFN-
401 λ 2 protein concentrations in cell lysates, were significantly greater following HRV-16 infection
402 than SARS-CoV-2 infection (**Panel C**, median increase expression 21.2-fold vs 4.3-fold,
403 $p < 0.0001$; **Panel D**, median 9848 pg/mL vs 7123 pg/mL, $p = 0.02$). Expression of *CXCL10*, and
404 CXCL10 protein concentrations in cell lysates, were significantly greater following HRV-16
405 infection as compared to SARS-CoV-2 infection (**Panel E**, median increase expression 9.8-fold
406 vs 5.4-fold, $p = 0.003$; **Panel F**, 69,306 pg/mL vs 15,232 pg/mL, $p < 0.0001$). Analyses by
407 Wilcoxon matched-pairs signed rank test. Bars indicate median values. Boxplots indicate
408 interquartile range and whiskers indicate minimum and maximum values.

409 **Figure 3.** Concentrations of secreted IFN β 1, IFN- λ 3, and CXCL10 (normalized to total protein
410 concentration) in the supernatant of primary bronchial epithelial cell cultures 48 hours and 96
411 hours after infection with SARS-COV-2 (red circles) or HRV-16 (blue triangles). Secreted IFN β 1
412 concentrations peaked at 48 hours post viral infection (**Panel A**), and IFN β 1 concentrations
413 were significantly higher in HRV-16 infected cultures than SARS-CoV-2 infected cultures at both
414 time points (**Panel A**). IFN- λ 3 (**Panel B**) and CXCL10 (**Panel C**) concentrations were also
415 significantly greater in HRV-16 infected cultures at 48 and 96 hours following infection.
416 * $p < 0.001$, ** $p = 0.005$, *** $p = 0.03$, **** $p = 0.04$, # $p = 0.2$. Analyses by Mann–Whitney tests.
417 Boxplots indicate interquartile range and whiskers indicate minimum and maximum values.

418 **Figure 4.** Correlation between relative gene expression of *IFNB1* or *IFNL2* (normalized to
419 GAPDH) and SARS-CoV-2 viral replication by quantitative PCR in primary bronchial epithelial
420 cell cultures in children (n=14) and adults (n=8). *IFNB1* and *IFNL2* gene expression were
421 inversely correlated with SARS-CoV-2 replication (**Panel A**, Spearman $r=-0.61$, $p=0.003$; **Panel**
422 **B**, Spearman $r=-0.42$, $p=0.05$).

423 **Figure 5.** Correlation between secreted IFN β 1 concentration 48 hours after SARS-CoV-2
424 infection or CXCL10 concentration from the cell lysate 96 hours after SARS-CoV-2 infection
425 (normalized to total protein concentration) and 96-hour replication of SARS-CoV-2 by
426 quantitative PCR in primary bronchial epithelial cell cultures in children (n=14) and adults (n=8).
427 Secreted IFN β 1 and SARS-CoV-2 replication were significantly inversely correlated (**Panel A**;
428 Spearman $r=-0.53$, $p=0.02$), and CXCL10 concentration from cell lysates was also significantly
429 inversely correlated with SARS-CoV-2 replication (**Panel B**; Spearman $r=-0.65$, $p=0.002$).

430 **Figure 6.** SARS-CoV-2 replication by quantitative PCR in primary bronchial airway epithelial
431 cell cultures from children (n=14) and adults (n=10) infected in parallel with SARS-CoV-2 alone
432 at MOI=0.5 (red circles), SARS-CoV-2 infection 72 hours following pre-infection with HRV-16
433 (MOI=0.5: blue triangles), pre- and concurrent treatment with recombinant IFN β 1 (orange
434 squares), and pre- and concurrent treatment with recombinant IFN λ 2 (green diamonds). Viral
435 copy number was quantified by PCR in RNA harvested 96 hours after SARS-CoV-2 infection.
436 Pre-infection of primary bronchial AECs with HRV-16 significantly reduced SARS-CoV-2
437 replication (median copy number 267,264 vs 14,788, p=0.002). Treatment of bronchial AEC
438 cultures with recombinant IFN β 1 or IFN λ 2 also significantly reduced SARS-CoV-2 replication
439 (median copy number 267,264 to 11,947, p=0.0001; median copy number 267,264 to 11,856,
440 p=0.0002, respectively). Kruskal–Wallis one-way ANOVA on ranks was used to compare all
441 experimental conditions. Dunn’s test was used for comparisons between SARS-CoV-2 alone
442 and individual experimental conditions. Bars indicate median values.

443 **Figure 7.** Relative gene expression of pattern-recognition receptor and RNA viral sensor *IFIH1*
444 (*MDA5*) (normalized to GAPDH expression) by primary bronchial airway epithelial cell cultures
445 in children (n=14) and adults (n=8). Gene expression was quantified by PCR in RNA harvested
446 96 hours after parallel infection with SARS-CoV-2 (MOI=0.5, red diamonds) or HRV-16
447 (MOI=0.5, blue diamonds). *IFIH1* expression was significantly higher after HRV-16 infection
448 than after SARS-CoV-2 infection ($p=0.003$ by Wilcoxon matched-pairs signed rank test; bars
449 indicate median values).

450 **REFERENCES:**

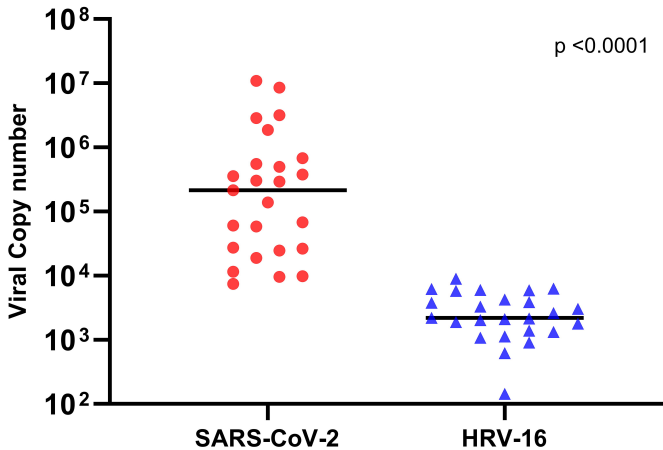
- 451 1. Medicine JHUa. Johns Hopkins University Coronavirus Resource Center - Mortality Analyses
452 [Website]. [Available from: <https://coronavirus.jhu.edu/data/mortality>.
453
- 454 2. Lai CC, Liu YH, Wang CY, Wang YH, Hsueh SC, Yen MY, et al. Asymptomatic carrier state, acute
455 respiratory disease, and pneumonia due to severe acute respiratory syndrome coronavirus 2 (SARS-CoV-
456 2): Facts and myths. *Journal of microbiology, immunology, and infection = Wei mian yu gan ran za zhi*.
457 2020.
458
- 459 3. Team CC-R. Severe Outcomes Among Patients with Coronavirus Disease 2019 (COVID-19) -
460 United States, February 12-March 16, 2020. *MMWR Morbidity and mortality weekly report*.
461 2020;69(12):343-6.
462
- 463 4. Cai J, Xu J, Lin D, Yang Z, Xu L, Qu Z, et al. A Case Series of children with 2019 novel coronavirus
464 infection: clinical and epidemiological features. *Clinical infectious diseases : an official publication of the*
465 *Infectious Diseases Society of America*. 2020.
466
- 467 5. Siegel DA, Reses HE, Cool AJ, Shapiro CN, Hsu J, Boehmer TK, et al. Trends in COVID-19 Cases,
468 Emergency Department Visits, and Hospital Admissions Among Children and Adolescents Aged 0-17
469 Years - United States, August 2020-August 2021. *MMWR Morbidity and mortality weekly report*.
470 2021;70(36):1249-54.
471
- 472 6. Sampaio NG, Chauveau L, Hertzog J, Bridgeman A, Fowler G, Moonen JP, et al. The RNA sensor
473 MDA5 detects SARS-CoV-2 infection. *Scientific reports*. 2021;11(1):13638.
474
- 475 7. Sa Ribero M, Jouvenet N, Dreux M, Nisole S. Interplay between SARS-CoV-2 and the type I
476 interferon response. *PLoS pathogens*. 2020;16(7):e1008737.
477
- 478 8. Park A, Iwasaki A. Type I and Type III Interferons - Induction, Signaling, Evasion, and Application
479 to Combat COVID-19. *Cell Host Microbe*. 2020;27(6):870-8.
480
- 481 9. Mazaleuskaya L, Veltrop R, Ikpeze N, Martin-Garcia J, Navas-Martin S. Protective role of Toll-like
482 Receptor 3-induced type I interferon in murine coronavirus infection of macrophages. *Viruses*.
483 2012;4(5):901-23.
484
- 485 10. Fung SY, Yuen KS, Ye ZW, Chan CP, Jin DY. A tug-of-war between severe acute respiratory
486 syndrome coronavirus 2 and host antiviral defence: lessons from other pathogenic viruses. *Emerging*
487 *microbes & infections*. 2020;9(1):558-70.
488
- 489 11. Mesel-Lemoine M, Millet J, Vidalain PO, Law H, Vabret A, Lorin V, et al. A human coronavirus
490 responsible for the common cold massively kills dendritic cells but not monocytes. *Journal of virology*.
491 2012;86(14):7577-87.
492
- 493 12. Lau SKP, Lau CCY, Chan KH, Li CPY, Chen H, Jin DY, et al. Delayed induction of proinflammatory
494 cytokines and suppression of innate antiviral response by the novel Middle East respiratory syndrome

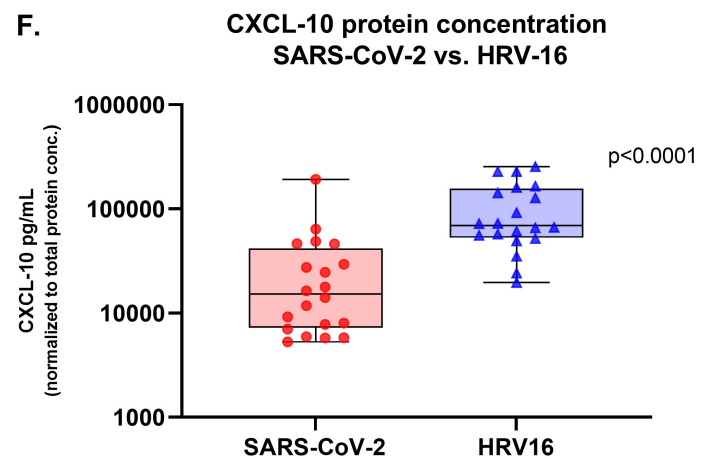
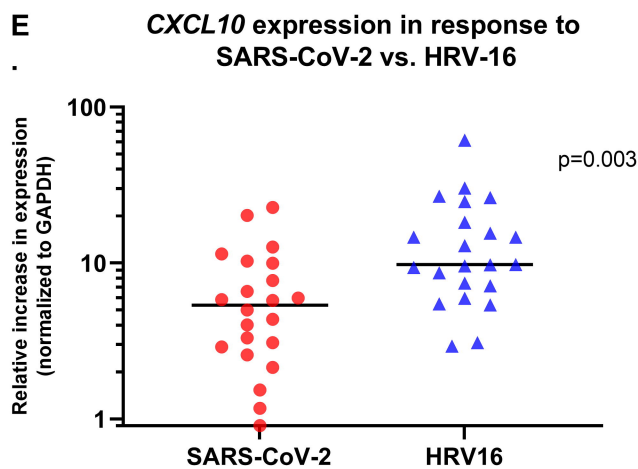
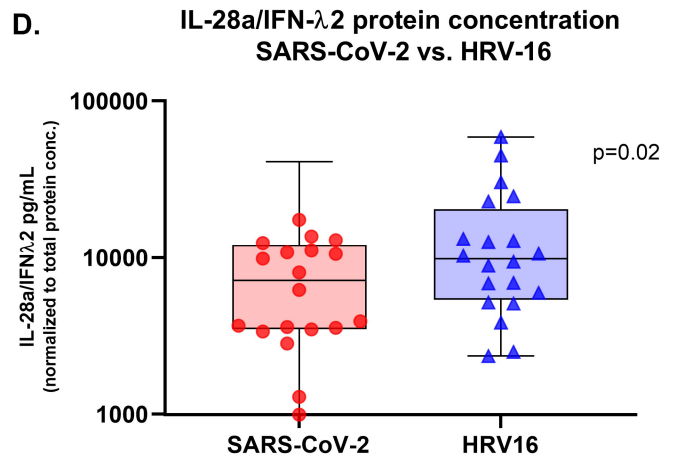
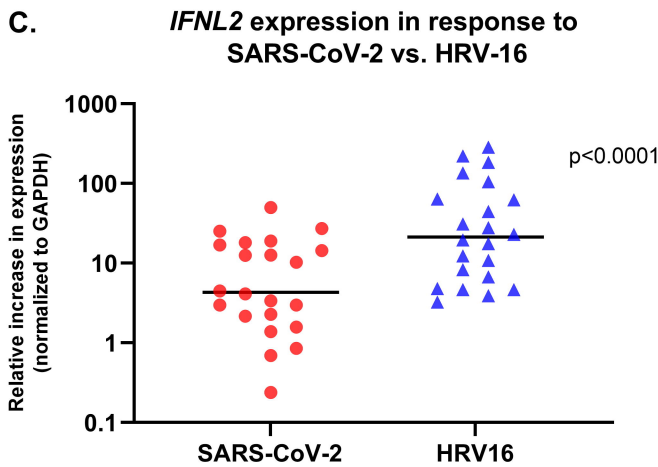
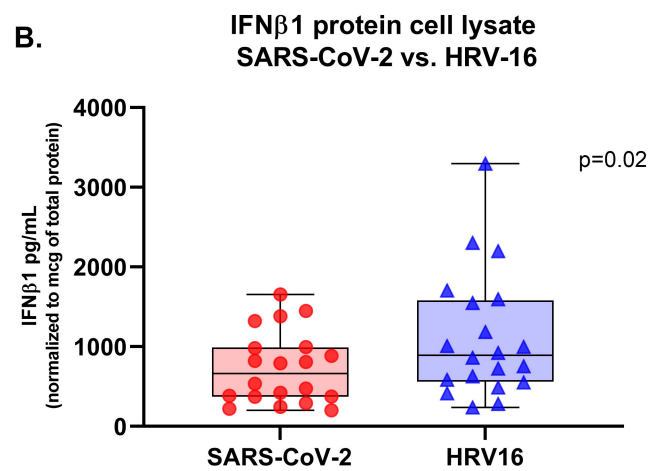
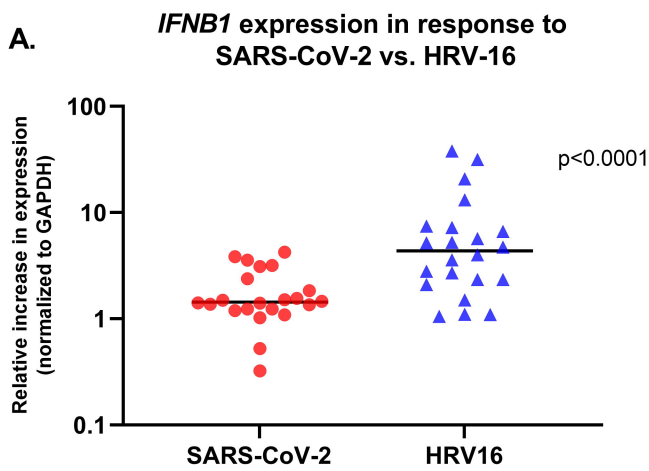
- 495 coronavirus: implications for pathogenesis and treatment. *The Journal of general virology*. 2013;94(Pt
496 12):2679-90.
497
- 498 13. Yoshikawa T, Hill TE, Yoshikawa N, Popov VL, Galindo CL, Garner HR, et al. Dynamic innate
499 immune responses of human bronchial epithelial cells to severe acute respiratory syndrome-associated
500 coronavirus infection. *PloS one*. 2010;5(1):e8729.
501
- 502 14. Niemeyer D, Mosbauer K, Klein EM, Sieberg A, Mettelman RC, Mielech AM, et al. The papain-like
503 protease determines a virulence trait that varies among members of the SARS-coronavirus species. *PLoS*
504 *pathogens*. 2018;14(9):e1007296.
505
- 506 15. Menachery VD, Gralinski LE, Mitchell HD, Dinnon KH, 3rd, Leist SR, Yount BL, Jr., et al. Middle
507 East Respiratory Syndrome Coronavirus Nonstructural Protein 16 Is Necessary for Interferon Resistance
508 and Viral Pathogenesis. *mSphere*. 2017;2(6).
509
- 510 16. Kindler E, Jonsdottir HR, Muth D, Hamming OJ, Hartmann R, Rodriguez R, et al. Efficient
511 replication of the novel human betacoronavirus EMC on primary human epithelium highlights its
512 zoonotic potential. *mBio*. 2013;4(1):e00611-12.
513
- 514 17. Sims AC, Tilton SC, Menachery VD, Gralinski LE, Schafer A, Matzke MM, et al. Release of severe
515 acute respiratory syndrome coronavirus nuclear import block enhances host transcription in human lung
516 cells. *Journal of virology*. 2013;87(7):3885-902.
517
- 518 18. Lei X, Dong X, Ma R, Wang W, Xiao X, Tian Z, et al. Activation and evasion of type I interferon
519 responses by SARS-CoV-2. *Nature communications*. 2020;11(1):3810.
520
- 521 19. Blanco-Melo D, Nilsson-Payant BE, Liu WC, Uhl S, Hoagland D, Moller R, et al. Imbalanced Host
522 Response to SARS-CoV-2 Drives Development of COVID-19. *Cell*. 2020;181(5):1036-45 e9.
523
- 524 20. Murphy RC, Lai Y, Barrow KA, Hamerman JA, Lacy-Hulbert A, Piliponsky AM, et al. Effects of
525 Asthma and Human Rhinovirus A16 on the Expression of SARS-CoV-2 Entry Factors in Human Airway
526 Epithelium. *American journal of respiratory cell and molecular biology*. 2020;63(6):859-63.
527
- 528 21. Ziegler CGK, Allon SJ, Nyquist SK, Mbanjo IM, Miao VN, Tzouanas CN, et al. SARS-CoV-2 Receptor
529 ACE2 Is an Interferon-Stimulated Gene in Human Airway Epithelial Cells and Is Detected in Specific Cell
530 Subsets across Tissues. *Cell*. 2020;181(5):1016-35 e19.
531
- 532 22. Zhang Q, Bastard P, Liu Z, Le Pen J, Moncada-Velez M, Chen J, et al. Inborn errors of type I IFN
533 immunity in patients with life-threatening COVID-19. *Science*. 2020;370(6515).
534
- 535 23. Meffre E, Iwasaki A. Interferon deficiency can lead to severe COVID. *Nature*.
536 2020;587(7834):374-6.
537
- 538 24. Hadjadj J, Yatim N, Barnabei L, Corneau A, Boussier J, Smith N, et al. Impaired type I interferon
539 activity and inflammatory responses in severe COVID-19 patients. *Science*. 2020;369(6504):718-24.
540
- 541 25. Ziegler CGK, Miao VN, Owings AH, Navia AW, Tang Y, Bromley JD, et al. Impaired local intrinsic
542 immunity to SARS-CoV-2 infection in severe COVID-19. *Cell*. 2021;184(18):4713-33 e22.

- 543 26. Vanderwall ERB, K.A.; Rich, L.M.; White, M.P.; Ziegler, S.F.; Rathe, J.A.; Debley, J.S. Interferon
544 Responses by Differentiated Primary Bronchial Airway Epithelial Cells to SarsCoV2 Are Less Robust Than
545 to Human Rhinovirus16. *American Journal of Respiratory and Critical Care Medicine*. 2021;203:A1292.
546
- 547 27. Lopez-Guisa JM, Powers C, File D, Cochrane E, Jimenez N, Debley JS. Airway epithelial cells from
548 asthmatic children differentially express proremodeling factors. *J Allergy Clin Immunol*. 2012;129(4):990-
549 7.
550
- 551 28. Reeves SR, Kolstad T, Lien TY, Elliott M, Ziegler SF, Wight TN, et al. Asthmatic airway epithelial
552 cells differentially regulate fibroblast expression of extracellular matrix components. *The Journal of*
553 *allergy and clinical immunology*. 2014;134(3):663-70 e1.
554
- 555 29. Altman MC, Reeves SR, Parker AR, Whalen E, Misura KM, Barrow KA, et al. Interferon response
556 to respiratory syncytial virus by bronchial epithelium from children with asthma is inversely correlated
557 with pulmonary function. *The Journal of allergy and clinical immunology*. 2018;142(2):451-9.
558
- 559 30. James RG, Reeves SR, Barrow KA, White MP, Glukhova VA, Haghghi C, et al. Deficient Follistatin-
560 like 3 Secretion by Asthmatic Airway Epithelium Impairs Fibroblast Regulation and Fibroblast-to-
561 Myofibroblast Transition. *American journal of respiratory cell and molecular biology*. 2018;59(1):104-13.
562
- 563 31. Barrow KA, Rich LM, Vanderwall ER, Reeves SR, Rathe JA, White MP, et al. Inactivation of
564 Material from SARS-CoV-2-Infected Primary Airway Epithelial Cell Cultures. *Methods Protoc*. 2021;4(1).
565
- 566 32. Pfaffl MW. A new mathematical model for relative quantification in real-time RT-PCR. *Nucleic*
567 *acids research*. 2001;29(9):e45.
568
- 569 33. Acharya D, Liu G, Gack MU. Dysregulation of type I interferon responses in COVID-19. *Nat Rev*
570 *Immunol*. 2020;20(7):397-8.
571
- 572 34. Channappanavar R, Fehr AR, Vijay R, Mack M, Zhao J, Meyerholz DK, et al. Dysregulated Type I
573 Interferon and Inflammatory Monocyte-Macrophage Responses Cause Lethal Pneumonia in SARS-CoV-
574 Infected Mice. *Cell Host Microbe*. 2016;19(2):181-93.
575
- 576 35. Liu G, Lee JH, Parker ZM, Acharya D, Chiang JJ, van Gent M, et al. ISG15-dependent activation of
577 the sensor MDA5 is antagonized by the SARS-CoV-2 papain-like protease to evade host innate immunity.
578 *Nat Microbiol*. 2021;6(4):467-78.
579
- 580 36. Snijder EJ, Limpens R, de Wilde AH, de Jong AWM, Zevenhoven-Dobbe JC, Maier HJ, et al. A
581 unifying structural and functional model of the coronavirus replication organelle: Tracking down RNA
582 synthesis. *PLoS Biol*. 2020;18(6):e3000715.
583
- 584 37. Romano M, Ruggiero A, Squeglia F, Maga G, Berisio R. A Structural View of SARS-CoV-2 RNA
585 Replication Machinery: RNA Synthesis, Proofreading and Final Capping. *Cells*. 2020;9(5).
586
- 587 38. Min YQ, Huang M, Sun X, Deng F, Wang H, Ning YJ. Immune evasion of SARS-CoV-2 from
588 interferon antiviral system. *Comput Struct Biotechnol J*. 2021;19:4217-25.
589

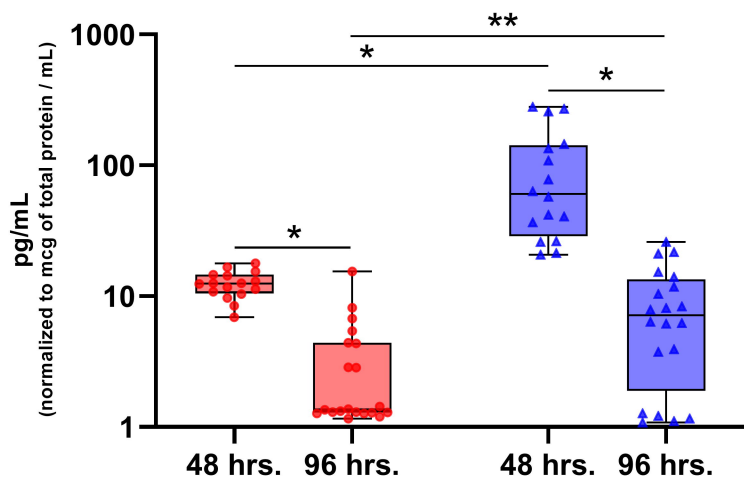
- 590 39. Scutigliani EM, Kikkert M. Interaction of the innate immune system with positive-strand RNA
591 virus replication organelles. *Cytokine Growth Factor Rev.* 2017;37:17-27.
592
- 593 40. Hackbart M, Deng X, Baker SC. Coronavirus endoribonuclease targets viral polyuridine
594 sequences to evade activating host sensors. *Proc Natl Acad Sci U S A.* 2020;117(14):8094-103.
595
- 596 41. Kindler E, Gil-Cruz C, Spanier J, Li Y, Wilhelm J, Rabouw HH, et al. Early endonuclease-mediated
597 evasion of RNA sensing ensures efficient coronavirus replication. *PLoS pathogens.* 2017;13(2):e1006195.
598
- 599 42. Deng X, Hackbart M, Mettelman RC, O'Brien A, Mielech AM, Yi G, et al. Coronavirus
600 nonstructural protein 15 mediates evasion of dsRNA sensors and limits apoptosis in macrophages. *Proc*
601 *Natl Acad Sci U S A.* 2017;114(21):E4251-E60.
602
- 603 43. Oh SJ, Shin OS. SARS-CoV-2 Nucleocapsid Protein Targets RIG-I-Like Receptor Pathways to Inhibit
604 the Induction of Interferon Response. *Cells.* 2021;10(3).
605
- 606 44. Guo G, Gao M, Gao X, Zhu B, Huang J, Luo K, et al. SARS-CoV-2 non-structural protein 13 (nsp13)
607 hijacks host deubiquitinase USP13 and counteracts host antiviral immune response. *Signal Transduct*
608 *Target Ther.* 2021;6(1):119.
609
- 610 45. Zheng Y, Zhuang MW, Han L, Zhang J, Nan ML, Zhan P, et al. Severe acute respiratory syndrome
611 coronavirus 2 (SARS-CoV-2) membrane (M) protein inhibits type I and III interferon production by
612 targeting RIG-I/MDA-5 signaling. *Signal Transduct Target Ther.* 2020;5(1):299.
613
- 614 46. Wu J, Shi Y, Pan X, Wu S, Hou R, Zhang Y, et al. SARS-CoV-2 ORF9b inhibits RIG-I-MAVS antiviral
615 signaling by interrupting K63-linked ubiquitination of NEMO. *Cell Rep.* 2021;34(7):108761.
616
- 617 47. Yuen CK, Lam JY, Wong WM, Mak LF, Wang X, Chu H, et al. SARS-CoV-2 nsp13, nsp14, nsp15 and
618 orf6 function as potent interferon antagonists. *Emerging microbes & infections.* 2020;9(1):1418-28.
619
- 620 48. Fu YZ, Wang SY, Zheng ZQ, Yi H, Li WW, Xu ZS, et al. SARS-CoV-2 membrane glycoprotein M
621 antagonizes the MAVS-mediated innate antiviral response. *Cell Mol Immunol.* 2021;18(3):613-20.
622
- 623 49. Wu Y, Ma L, Zhuang Z, Cai S, Zhao Z, Zhou L, et al. Main protease of SARS-CoV-2 serves as a
624 bifunctional molecule in restricting type I interferon antiviral signaling. *Signal Transduct Target Ther.*
625 2020;5(1):221.
626
- 627 50. Shin D, Mukherjee R, Grewe D, Bojkova D, Baek K, Bhattacharya A, et al. Papain-like protease
628 regulates SARS-CoV-2 viral spread and innate immunity. *Nature.* 2020;587(7835):657-62.
629
- 630 51. Klemm T, Ebert G, Calleja DJ, Allison CC, Richardson LW, Bernardini JP, et al. Mechanism and
631 inhibition of the papain-like protease, PLpro, of SARS-CoV-2. *EMBO J.* 2020;39(18):e106275.
632
- 633 52. Jiang HW, Zhang HN, Meng QF, Xie J, Li Y, Chen H, et al. SARS-CoV-2 Orf9b suppresses type I
634 interferon responses by targeting TOM70. *Cell Mol Immunol.* 2020;17(9):998-1000.
635
- 636 53. Gordon DE, Jang GM, Bouhaddou M, Xu J, Obernier K, White KM, et al. A SARS-CoV-2 protein
637 interaction map reveals targets for drug repurposing. *Nature.* 2020;583(7816):459-68.

- 638 54. Miorin L, Kehrer T, Sanchez-Aparicio MT, Zhang K, Cohen P, Patel RS, et al. SARS-CoV-2 Orf6
639 hijacks Nup98 to block STAT nuclear import and antagonize interferon signaling. *Proc Natl Acad Sci U S*
640 *A.* 2020;117(45):28344-54.
641
- 642 55. Xia H, Cao Z, Xie X, Zhang X, Chen JY, Wang H, et al. Evasion of Type I Interferon by SARS-CoV-2.
643 *Cell Rep.* 2020;33(1):108234.
644
- 645 56. Mu J, Fang Y, Yang Q, Shu T, Wang A, Huang M, et al. SARS-CoV-2 N protein antagonizes type I
646 interferon signaling by suppressing phosphorylation and nuclear translocation of STAT1 and STAT2. *Cell*
647 *Discov.* 2020;6:65.
648
- 649 57. Naslavsky MS, Vidigal M, Matos L, Coria VR, Batista Junior PB, Razuk A, et al. Extreme
650 phenotypes approach to investigate host genetics and COVID-19 outcomes. *Genet Mol Biol.* 2021;44(1
651 *Suppl 1)*:e20200302.
652
- 653 58. Cheemarla NR, Watkins TA, Mihaylova VT, Wang B, Zhao D, Wang G, et al. Dynamic innate
654 immune response determines susceptibility to SARS-CoV-2 infection and early replication kinetics. *J Exp*
655 *Med.* 2021;218(8).
656
- 657 59. Dee K, Goldfarb DM, Haney J, Amat JAR, Herder V, Stewart M, et al. Human Rhinovirus Infection
658 Blocks Severe Acute Respiratory Syndrome Coronavirus 2 Replication Within the Respiratory Epithelium:
659 Implications for COVID-19 Epidemiology. *The Journal of infectious diseases.* 2021;224(1):31-8.
660
- 661 60. Monk PD, Marsden RJ, Tear VJ, Brookes J, Batten TN, Mankowski M, et al. Safety and efficacy of
662 inhaled nebulised interferon beta-1a (SNG001) for treatment of SARS-CoV-2 infection: a randomised,
663 double-blind, placebo-controlled, phase 2 trial. *The Lancet Respiratory medicine.* 2021;9(2):196-206.
664

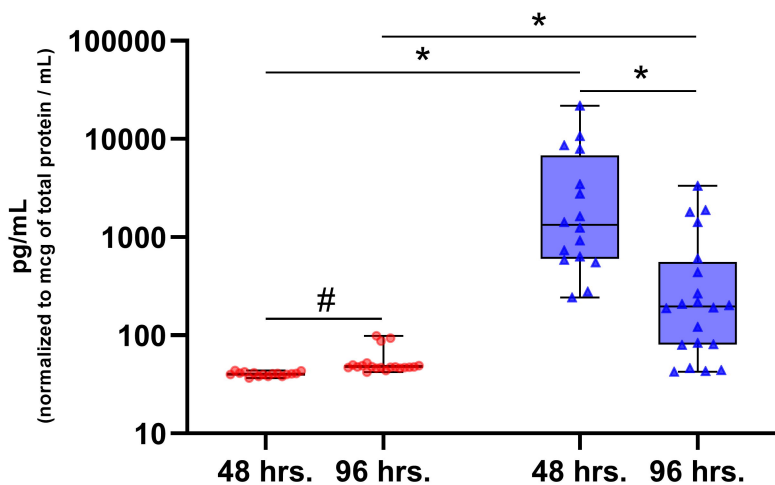




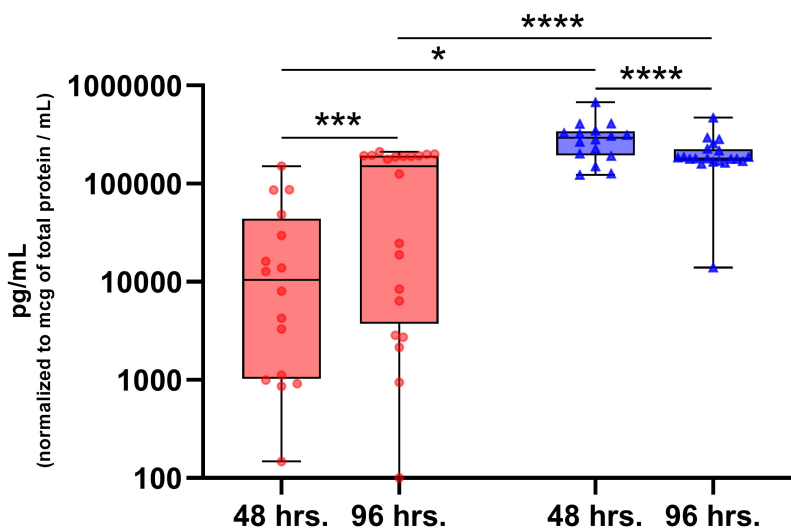
A. Secreted IFN β 1



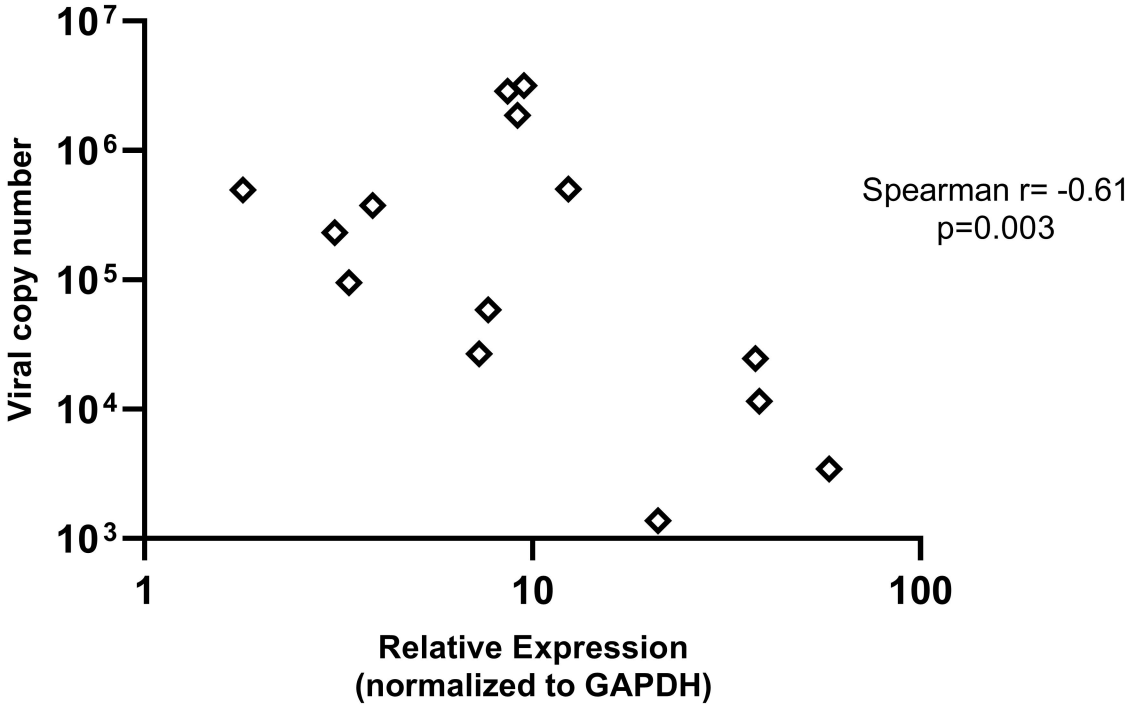
B. Secreted IFN λ 3



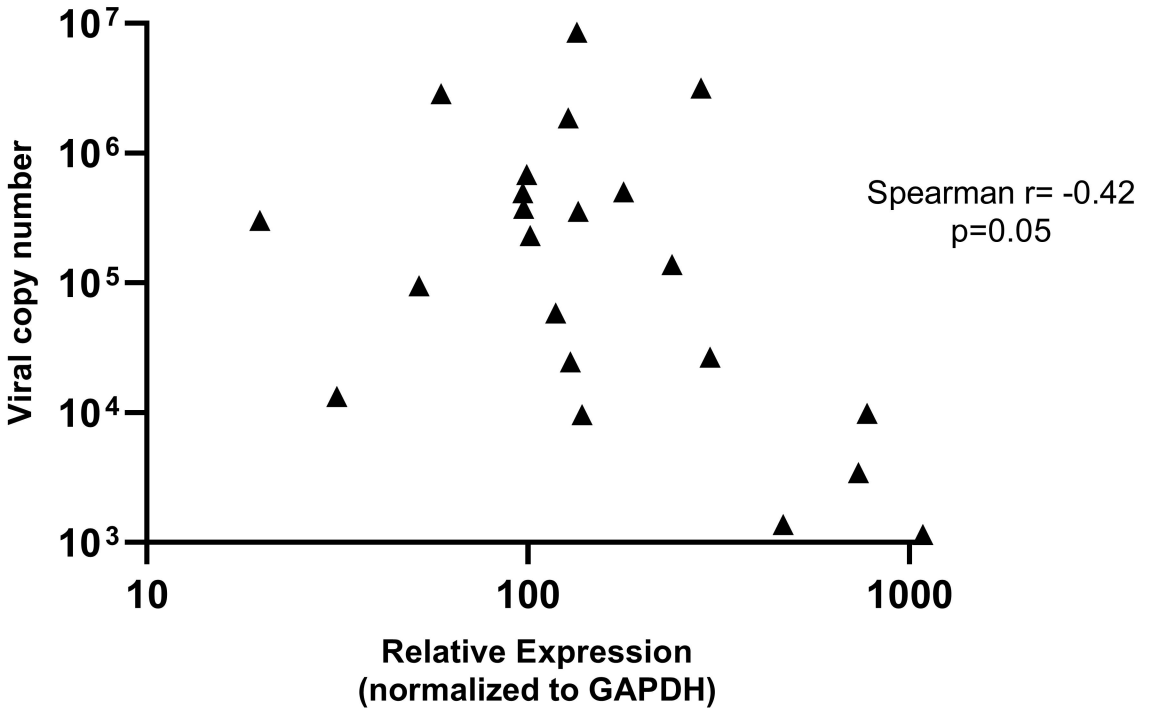
C. Secreted CXCL10



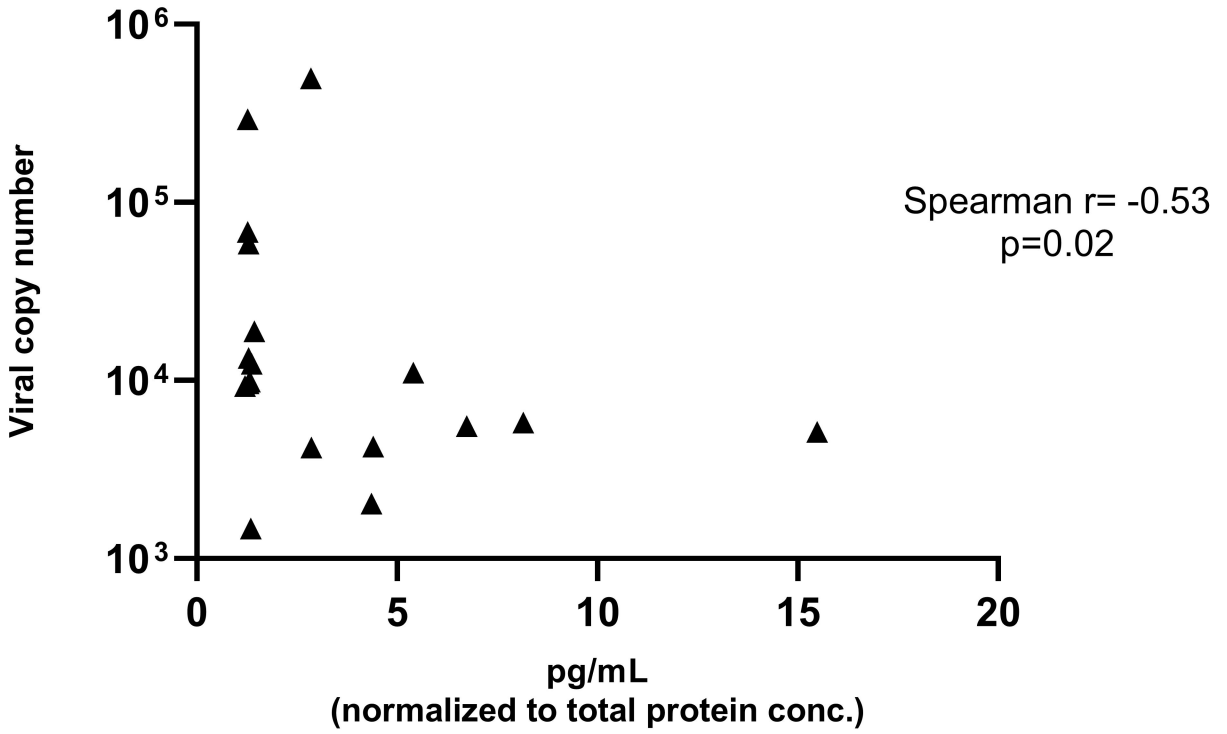
A. Correlation between *IFNB1* expression and SARS-CoV-2 replication (96hrs.)



B. Correlation between *IFNL2* expression and SARS-CoV-2 replication (96hrs.)



A. Correlation between IFN β 1 protein in supernatant (48hrs.) and SARS-CoV-2 replication



B. Correlation between CXCL10 protein in cell lysate and SARS-CoV-2 replication

